ISSN 0031-918X, Physics of Metals and Metallography, 2019, Vol. 120, No. 8, pp. 796–805. © Pleiades Publishing, Ltd., 2019.
Published in Russian in Fizika Metallov i Metallovedenie, 2019, Vol. 120, No. 8, pp. 867–877.

STRENGTH AND PLASTICITY

Characterization of Microstructure and Mechanical Properties of Multilayer Al/Cu/Mg/Ni Composite Produced through Accumulative Roll Bonding

S. Shakouri[a] and B. Eghbali[a, *]

[a]*Department of Materials Science Engineering, Sahand University of Technology, P.O. Box 51335-1996, Tabriz, Iran*
**e-mail: eghbali@sut.ac.ir*

Received January 17, 2018; revised March 21, 2018; accepted March 25, 2019

Abstract—In this research, Al/Cu/Mg/Ni multilayer composite was produced by accumulative roll bonding process. Microstructure evolution and mechanical properties of the composites are evaluated within different cycles of accumulative roll bonding process. Optical microscope images showed that after six accumulative roll bonding cycles, a multilayer Al/Cu/Mg/Ni composite with homogenously distributed fragmented Cu, Mg, and Ni layer particles in Al matrix was achieved. With increasing the accumulative strain, the strength and elongation of the composites increased. Also, the measurement of specific strength which is defined as strength-to-density ratio showed that specific strength of the composite has become about 3.25 times higher than that of matrix metal (Al). Fracture mode has changed from normal in the primary sandwich to normal-and-shear in 6th accumulative roll bonding cycle, and due to the observed dimples in both conditions, it can be concluded that fracture mode in the composites was ductile.

Keywords: multilayer Al/Cu/Mg/Ni composites, accumulative roll bonding, mechanical properties, severe plastic deformation, deformation bonding

DOI: 10.1134/S0031918X19080143

1. INTRODUCTION

The techniques of severe plastic deformation (SPD) which can be explained as deformation to large strains below recrystallization temperatures have been of continual interest in production of novel metallic microstructures [1, 2]. Several novel techniques have been developed to create high strain in metals without changes in initial sample dimensions, such as equal-channel angular pressing (ECAP) [3], high-pressure torsion (HPT) [3], multi-axial forging (MAF) [4], and accumulative roll bonding (ARB) [3, 5]. Among these processes, the ARB process is a relatively new method of severe plastic deformation which is proposed by Saito et al. [6] and has several advantages over other SPD processes such as: (i) forming facilities with large load capacity and expensive dies are not needed, (ii) high productivity rate, and (iii) the amount of material to be produced is not limited [2]. The basic goal of ARB is to impose an extremely high plastic strain on the material, which results in structural refinement and strength increase without changing specimen dimensions. Moreover, in order to obtain one-body solid material of original sheets, ARB is not only a deformation process but also a bonding process (roll bonding) [2]. To achieve a good bonding of metallic sheets, the sheet surfaces are subjected to surface treatments before stacking, such as degreasing and wire brushing. The length of roll bonded material is then sectioned into two halves. The sectioned sheets are again surface treated, stacked, and roll bonded [5]. Lots of researchers have been carried out fabrication of different composites by using ARB process. Recently, Shabani and et al. fabricated Al/Ni/Cu composite using ARB and electroplating process [6]. It is seen that with increasing the ARB cycles the tensile strength of composite improved and after eleven cycles, a composite of Al matrix with uniform distribution of reinforcing phases (Ni and Cu) produced. Brunelli et al. have produced Al/Ni multilayered composite by ARB [7]. They have shown that the prolonged heat treatment from 500 to 600°C allows the formation of different Al–Ni intermetallic phases. Ghalandari et al. processed Cu/Zn multilayer composite via ARB technique [8]. The microstructural evolution of produced composite has been correlated to mechanical properties achieved. As was reported, after four cycles necking started at various locations in the microstructure and the interfaces become wavy. During ARB, the Kirkendall porosities were formed in Zn layer. Other researchers [9] fabricated nanolamellar Cu–Nb multilayers composites via combination of ARB and rolling. The results displayed the texture evolution of Cu and Nb in the processed composite. TEM and SEM indicated the onset of various defor-

Table 1. Specifications and mechanical properties of commercially pure sheets used in the study

Materials	Sheet dimensions (l, w, t), mm	Hardness, VHN	Elongation, %	Yield strength, MPa
Al-annealed	90 × 45 × 1	35	42	28
Cu-annealed	90 × 45 × 0.5	64	45	69
Mg-annealed	90 × 45 × 0.5	32	10	75
Ni-annealed	90 × 45 × 0.5	107	40	70

mation modes such as shear banding and twinning. The Al/Mg was multilayered with the good interface bond strength and no diffusion layer at interface has been produced by ARB [10]. It has been seen that with increasing the ARB pass the grain size of the composite refines to sub-micrometer scale. Talebian and Alizadeh [11] have been processed Al/steel multilayered composite by using ARB. They have found that because of the difference between the flow properties of the Al layer and steel layer the necking and rupture of the steel layers took place in the second cycle. The annealing treatment at 500°C leads to the formation of the intermetallic phases at the interfaces of Al and steel layers. Therefore, it is seen that only a few attempts have been made to fabricate tri-metallic multilayer composites. In addition, there are no works reporting the synthesis, microstructure, and mechanical properties of four-metallic multilayer composites fabricated from four different metals. Moreover, among four-metallic systems, the microstructure development and mechanical properties of Al/Cu/Mg/Ni dissimilar metals combination have not yet been investigated. Accordingly, in the present research, multilayered Al/Cu/Mg/Ni composite is processed by ARB. The evolution of the microstructure and its influence on the mechanical properties is examined and the results are discussed.

2. EXPERIMENTAL

2.1. Research Material

In this study, strips of commercial pure Al, Cu, Mg, and Ni were used as raw materials. Table 1 shows the properties of these materials. Before using these sheets as the starting materials, they were all subjected to full annealing. Table 2 shows time periods and temperatures at which annealing of the sheets were performed. Annealing parameters are selected based on previous researcher's experiences [6, 11–14].

2.2. Accumulative Roll Bonding of the Composites

Figure 1 shows schematics of ARB process that was used for preparing the composites. Sheets with presented dimensions in Table 1 were cut from annealed stock sheets and were degreased in acetone. In order to obtain a good bonding of metal sheets, scratch brushing with a 90-mm-diameter circular stainless steel brush with 0.2 mm wire diameter was performed. Then, in order to avoid sliding of the strips on each other, they were alternatively stacked together and fastened by steel wires at four corner points. Primary sandwich was produced with 7 layers in total primary thickness of 5.5 mm (2 Al sheets on top and down of specimen, and 2 Al sheets between Cu, Mg, and Ni sheets) and was held for 10 minutes at 100°C in a preheated furnace and then was rolled down to a thickness of 2.0 mm without lubrication. Therefore, thickness reduction in primary sandwich was equal to approximately 63%. Rolling of composites was performed with a 350 mm roll diameter, which had a loading capacity of 30 tons. Rolling speed was set to 10 rpm. According to Fig. 1, primary sandwiches with thickness of 2 mm were cut into two halves, degreased in acetone, wire brushed, stacked together with steel wires in four corners, and rolled to 50% reduction in thickness after preheating for 10 min at 100°C, respectively. This process was repeated up to six cycles and corresponded to equivalent Von-Mises strain of 4.8 (0.8 for each cycle). According to 50% reduction in each cycle of ARB, accumulative strain can be measured as [6]:

$$\varepsilon_t = \left\{\frac{2}{\sqrt{3}}\ln\left(\frac{1}{2}\right)\right\} \times n = 0.8n,$$

where ε_t and n are the accumulative strain and number of applied ARB cycles, respectively.

2.3. Metallographic Procedure

In order to evaluate microstructural variations in various ARB cycles, an optical microscope (OM) and a scanning electron microscope (SEM-CAMSCAN MV2300) were employed. OM observations were per-

Table 2. Annealing conditions for commercially pure metallic sheets

Materials	Time period, min	Temperature, °C
Al	120	400
Cu	120	500
Mg	120	390
Ni	140	720

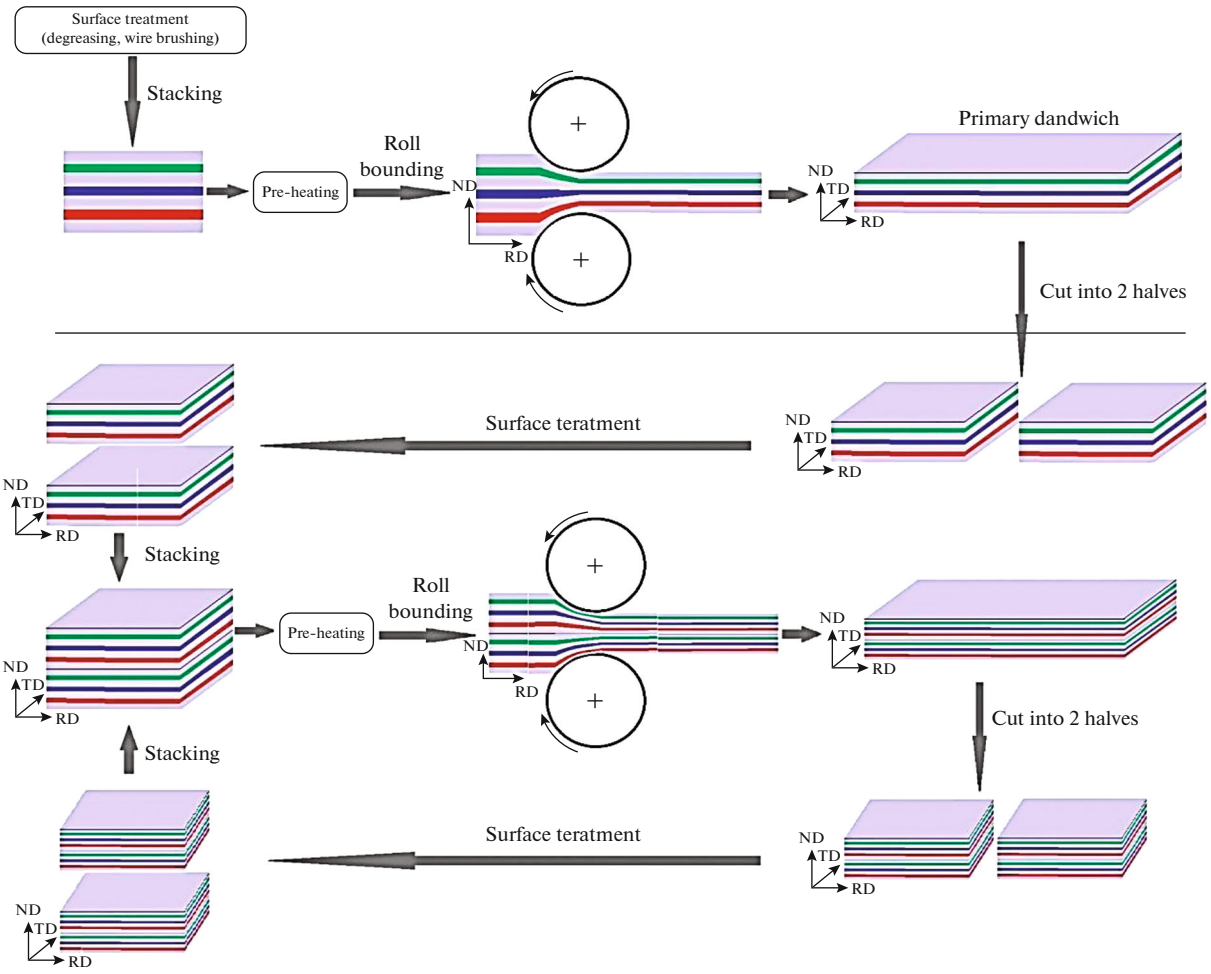

Fig. 1. Schematics of ARB process used for preparation of primary sandwich and cycles of ARB process.

formed on rolling direction-normal direction plane (RD-ND) of the roll bonded sheets. Prior to metallographic investigations, samples were mounted and their surface was sandpapered and polished, respectively. Ethyl alcohol and 5% Al_2O_3–5 μm solution was used for the last polishing step. Chemical composition gradients of interface layers were determined by an EDX spectrometer.

2.4. X-Ray Diffraction Analysis

The X-ray diffraction technique was used for phase identification of produced composites. Diffraction patterns were recorded using a Philips Bruker diffractometer (Model PW1800) employing Cu $K\alpha$ at room temperature. The data were collected for diffraction angles $35° \le 2\theta \le 105°$, with a step width of 0.05° and a step time of 1 s. Diffraction was performed on the cross-sections of 2 samples which are primary and 6th cycle samples. Image analysis method was used to evaluate variation of layer thickness in Cu, Mg, and Ni layers through different ARB cycles, and to this end, Clemex Vision PE software (Ver 3.5-2002) was made use of.

2.5. Investigation of Mechanical Properties

In order to investigate mechanical properties of Al/Cu/Mg/Ni composites, tensile and microhardness tests were performed. A Zwick Roell (Model Z010) tensile machine at a strain rate of $1.4 \times 10^{-4}\ s^{-1}$ at room temperature was employed. As shown in Fig. 2, the gauge length and width of tensile test specimens were 10 and 3, respectively, which correspond to measured dimensions according to standard no. 7 JIS-Z2201. Corresponding standard dimensions and related measurements are presented in Table 3. For each testing conditions, namely, each ARB cycle, 3 tensile samples were prepared. The reported values for strain and stress are mean of measured values in tensile tests with less than 2% error. Vickers microhardness was performed by a LECO-M400 apparatus under a load of 25 g and a time of 10 s on composites' cross-sections,

perpendicular to the rolling direction. A mean value of three points is reported for Vickers microhardness.

3. RESULTS AND DISCUSSION

3.1. Effect of ARB Cycles on the Microstructural Evolutions

Figure 3 illustrates microstructure variations of Al/Cu/Mg/Ni composites during different ARB cycles in RD-ND plane. It is obvious that the layers were uniform and coherent just as in primary sandwich (Fig. 3a). As is shown in Fig. 3b, Ni was the first layer that initiated necking and fracture locally (shown by red arrows) and this segregation occurred at first ARB cycle. Similarly, necking occurred in Cu layers at 2nd cycle of ARB (shown by red arrow in Fig. 3c) but fractured at subsequent cycle. Because of lower work-hardenability of Mg compared to Ni and Cu, the continuity of these layers maintained up to 3rd cycle (Fig. 3d). Thus, Mg was necked in 3rd and fractured at 4th cycle of ARB (Fig. 3e). In several studies, it is reported that during co-deformation of dissimilar attached metals in ARB process, the harder metal layer necks and fractures first [12–14]. The result of current study is in agreement with this phenomenon. As is seen, necking and fracturing is occurred in Ni, Cu, and Mg layers, respectively. It should be noted that the selected part of the metallographic image from OM analysis had a repeated pattern in the whole microstructure, especially in Fig. 3g. Thus, although Ni phase has a random distribution in Fig. 3g, in the higher scale, Ni has a semi-uniform distribution in the microstructure, totally. So, finally after six ARB cycles a composite with homogeneously distributed reinforcement particles, i.e. Cu–Mg–Ni fragments, was achieved. Accordingly, it is seen that an Al/Cu/Mg/Ni multilayer composite with uniform distribution of fragments will be achieved, if the multilayer is conducted to relatively high number of ARB cycles. Chemical composition gradients of interface layers determined by an EDX spectrometer are shown in Fig. 4. As can be seen from Figs. 4a–4f, the EDS line scan shapes displays that interdiffusion of Al/Cu, Al/Mg, and Al/Ni atoms occurred at the interfaces. Figures 4a–4c show that in primary sandwiches no diffusion layer at interfaces has been produced. But the atoms diffusion is relatively higher in 6th ARB cycle processed composite (Figs. 4d, 4e, and 4f) in comparison to primary sandwiches. Subsequently, a homogeneous bonding could be obtained. As is reported in

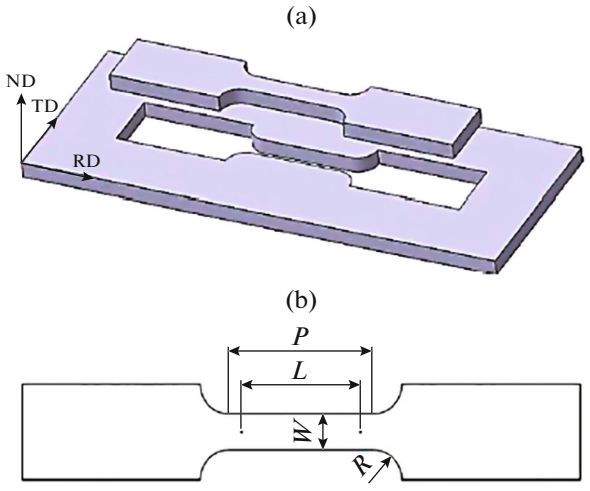

Fig. 2. Schematics of tension specimens produced from composites by wire cutting through (a) rolling direction, and (b) dimensional specifications.

[15, 16], increasing ARB cycles causes deformation-induced interdiffusion with the elimination of voids in the interfaces. In Fig. 5, the XRD patterns for the Al/Cu/Mg/Ni multilayer composite subjected to six cycles are shown. As can be seen, only Al, Cu, Mg, and Ni are distinguished in the patterns and the important feature of the patterns is that no intermetallic compound was formed during 6 cycles of ARB.

Figure 6 illustrates variation of Cu, Mg, and Ni layer thickness through RD-ND direction of OM microstructures in 2nd, 4th, and 6th ARB cycles, respectively. This variation data were collected from microstructure using image analysis software that is introduced above. It is obvious that as ARB cycles number increase, thickness of all layers decreases and the amount of this variant depends upon workability of layers. Compared to Cu and Mg, due to higher work hardening coefficient in Ni layers, it can be seen that beside high amount of deformation occurred in Cu and Mg, Ni layers resisted to high deformation. Thus at early cycles, compared to Cu and Mg, variation of Ni layer is low.

In Fig. 7, mean thickness variations of Cu, Mg, Ni layers versus the number of ARB cycles are shown. As is seen, a rapid decrease in average thickness of Ni, Mg, and Cu layers is occurred with increasing of ARB cycles to 3. But, by further increasing of ARB cycles the rate of decreasing in thickness is reduced.

Table 3. Specification of tension test specimens (adapted from standard no. 7 JIS-Z2201)

Width W, mm	Gauge Length L, mm	Parallel Length P, mm	Radius of Fillets R, mm	Thickness T, mm
3	$4\sqrt{A} = 10$	$\sim 1.2L = 12$	25	2.1

A: cross section area of parallel portion ($T \times W$)

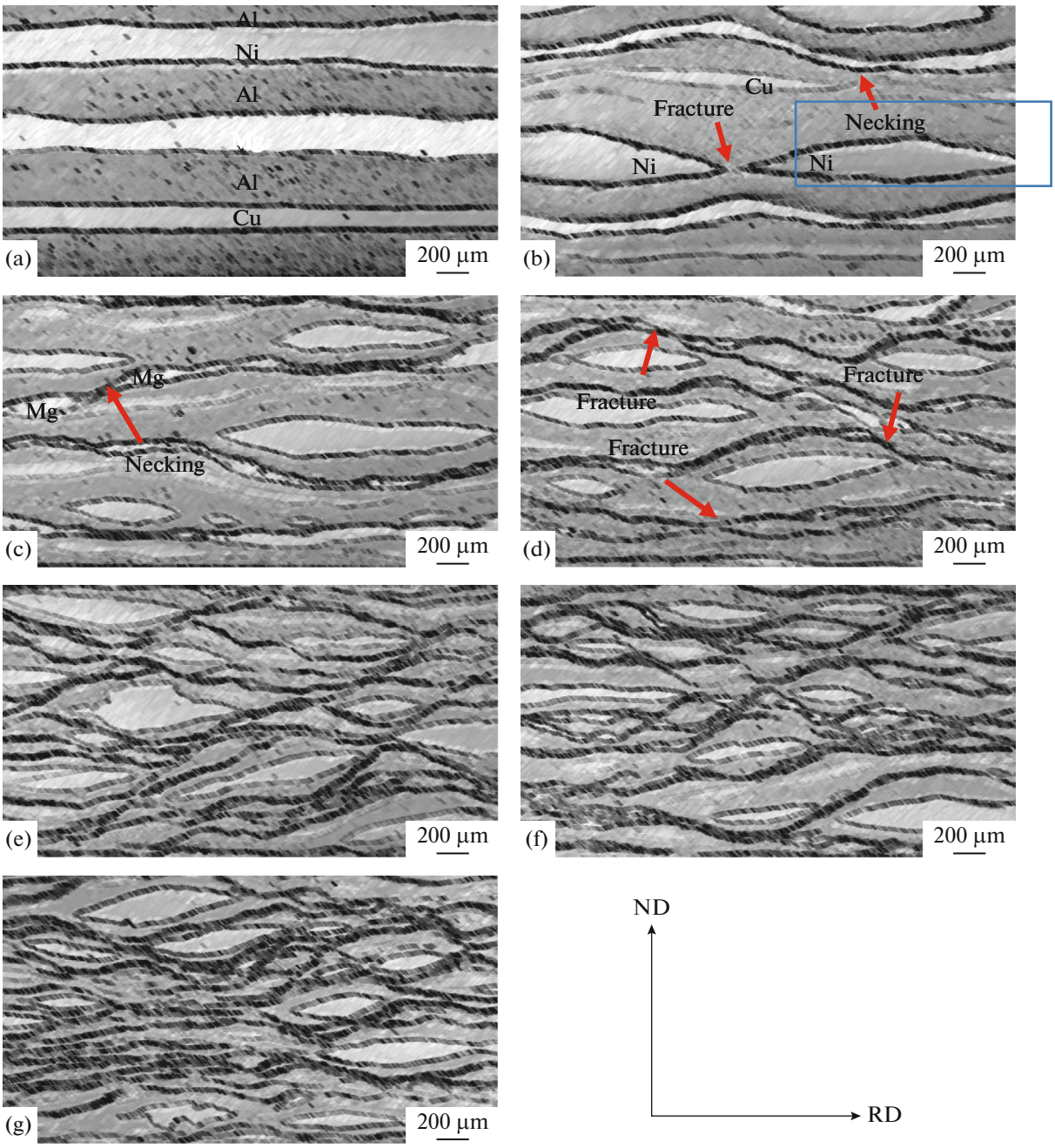

Fig. 3. Microstructural evolutions during ARB cycles, (a) primary sandwich, (b) first cycle, (c) 2nd, (d) 3rd, (e) 4th, (f) 5th, and (g) 6th cycle.

Decreasing in layers thickness is attributed to strain increasing by increasing the number of ARB cycles [6]. The fracture of layers after third cycle caused a reducing in the rate of layers thickness decreasing. Also, it is seen that mean layer thickness of Ni is higher than that of Cu and Mg. This phenomenon also could be understood from microhardness data discussed in the next section.

3.2. Evaluation of Mechanical Properties

Figure 8 illustrates the microhardness variations of different composite layers from primary sandwich to 6th ARB cycle. It is obvious that the microhardness in all layers has increased rapidly at primary cycles and after first cycle it has reached a plateau type. As a result, dislocation density has increased at primary and first ARB cycle rapidly, and it has reached a satu-

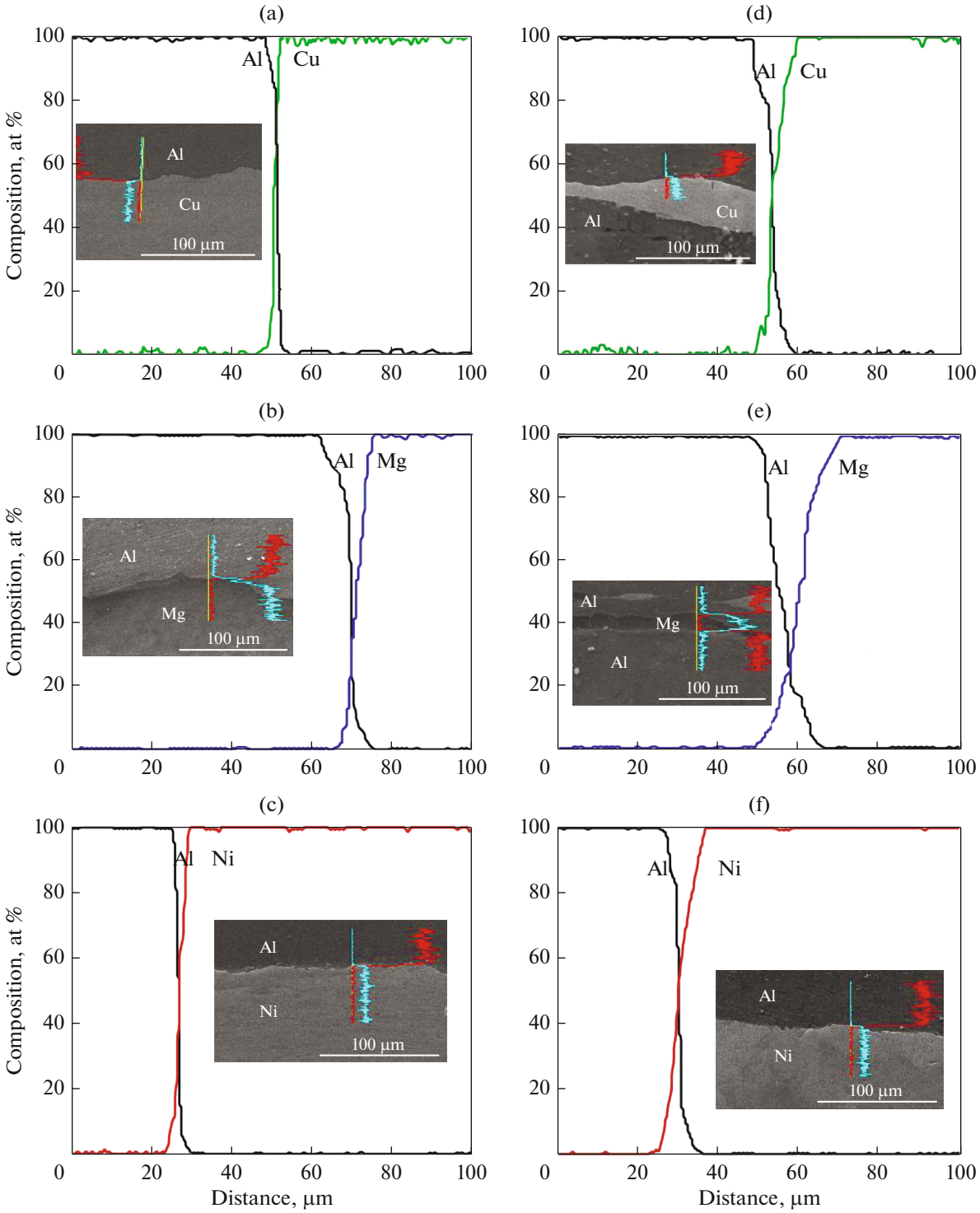

Fig. 4. EDX spectrometer analysis showing diffusion of couples in interfaces of primary sandwich: (a) Al–Cu, (b) Al–Mg, and (c) Al–Ni, and 6th ARB cycle composite layers: (d) Al–Cu, (e) Al–Mg, and (f) Al–Ni.

rated state after first cycle, i.e. due to preheating and adiabatic heating of specimens during plastic deformation, dislocations move easily and production and elimination of dislocations occur increasingly [17]. Because of increasing dislocation density, this phenomenon could be related to strain hardening of metal layers during plastic deformation [7]. It is clear that by increasing ARB cycles, microhardness of Ni layer increases with higher rate compared to that of the other three layers. This is due to the effect of plastic

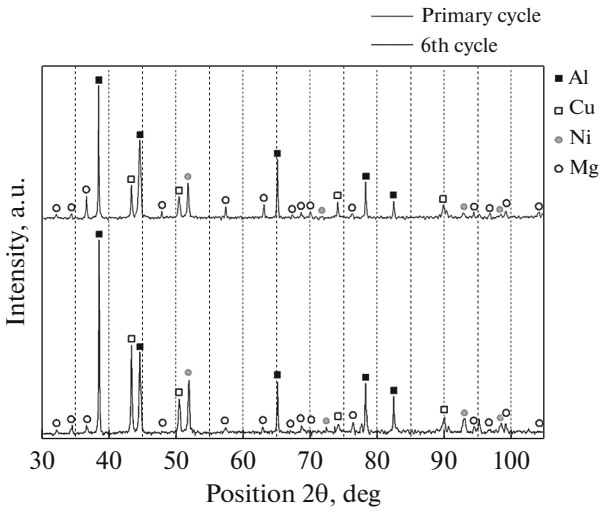

Fig. 5. XRD patterns of 6th cycle ARBed Al/Cu/Mg/Ni multilayer composites.

deformation that has significant effect on hardening or strengthening of metals. It is seen that the hardness variation trend of the Ni and other three layers with the ARB pass is remarkably different. After the first ARB cycle, the hardness of the Ni and Cu layers increases up to about 2.4 and 2.1 times that of the initial sheets, respectively. While that of the Al and Mg layers are improved only slightly. This shows that the first ARB cycle is the key strengthening stage for the Ni and Cu layers in the composite due to the rapid increase in the dislocation density [10, 18, 19], and that results in the increase in the hardness of Ni and Cu. But at higher number of ARB cycles, Hall-Petch effect favors work hardening and as is mentioned in previous studies [15, 16] this effect has lower rate of hardening than work-hardening induced by severe plastic deformation.

The engineering stress-strain curves of multilayer composite for various ARB cycles are shown in Fig. 9. It is seen that with increasing of ARB cycles the yield and the ultimate tensile strength of the composites are remarkably higher than that of primary sandwich.

At the first ARB cycle, both engineering yield strength and ultimate tensile strength are decreased. This is because of cracking and partitioning of reinforcing layers in the Al matrix, especially Ni and Cu layers. The maximum tensile strength was reached to about 265 MPa at the six ARB cycles. As reported, the yield and tensile strength of multilayer metallic composites depends on the tensile properties of the component parts and work hardening behavior of the soft part [18]. During ARB of metals, two key strengthening mechanisms are recognized [20, 21]: strain hardening by dislocation generation and grain refinement.

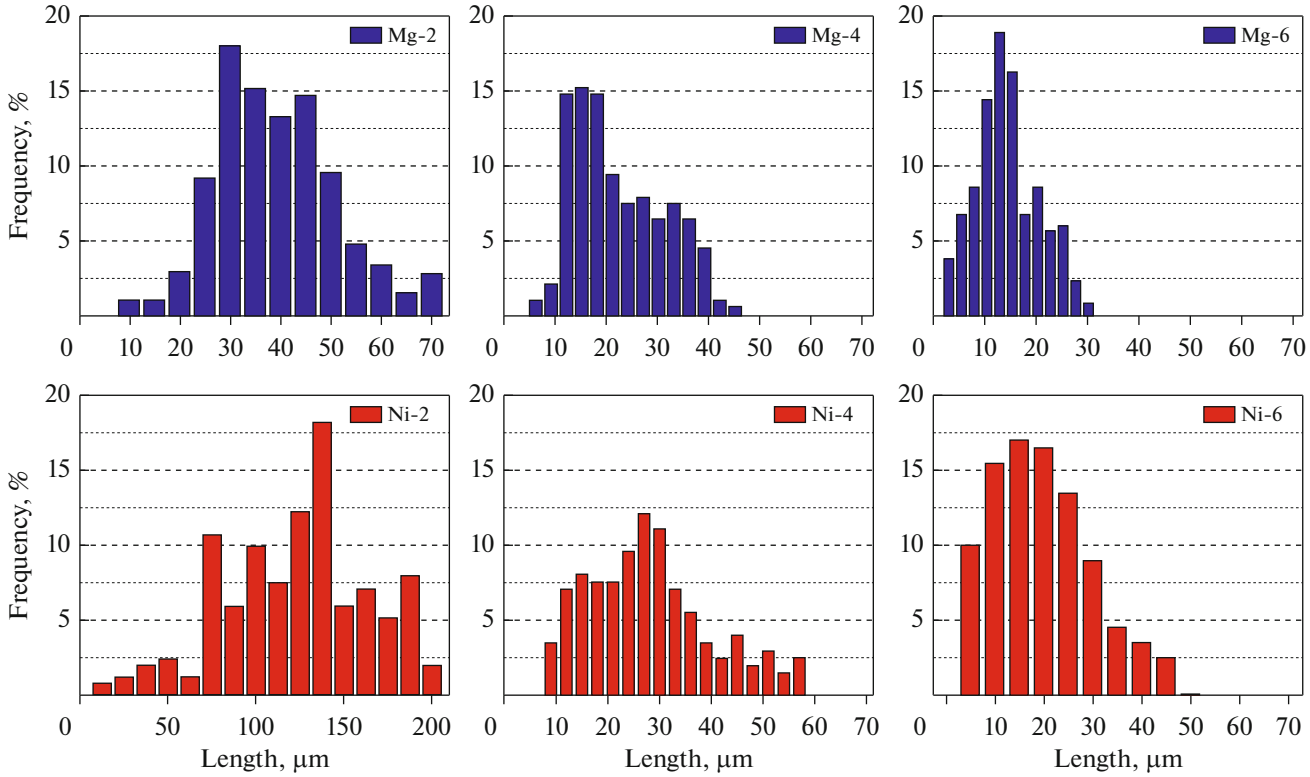

Fig. 6. Variation of Cu, Mg, and Ni layers thickness during 2nd (left column), 4th (mid column), and 6th (right column) cycle of ARB process (data collected from image analysis software Clemex Vision PE-2002).

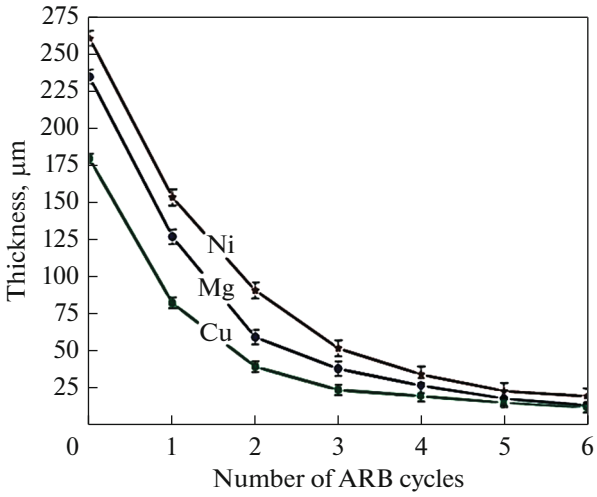

Fig. 7. Mean layer thickness variation of Cu, Mg, Ni particles during different ARB cycles.

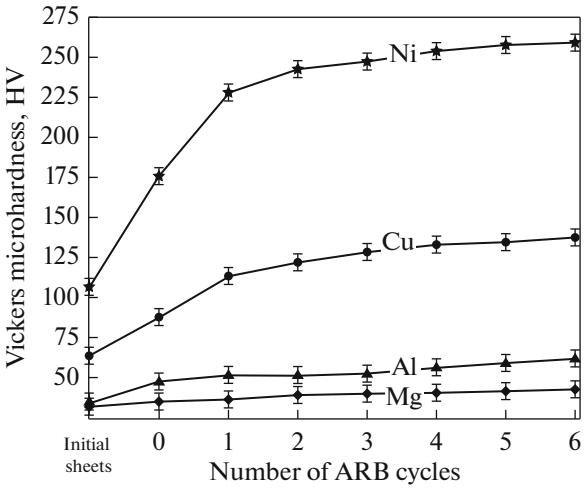

Fig. 8. Vickers microhardness variations vs. number of ARB cycles for different composite layers.

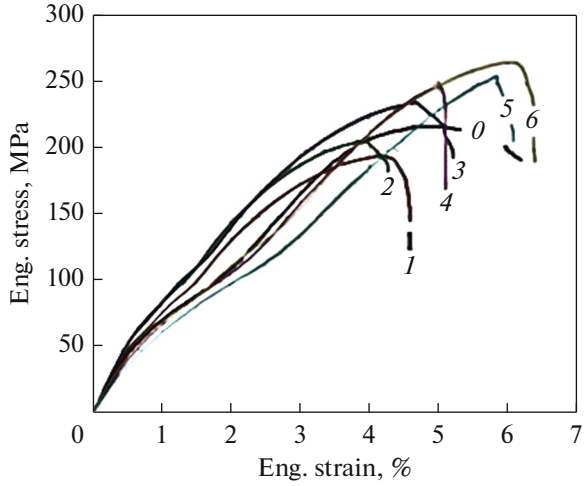

Fig. 9. Engineering stress vs. engineering strain curves (tension behavior) of composites during various ARB cycles.

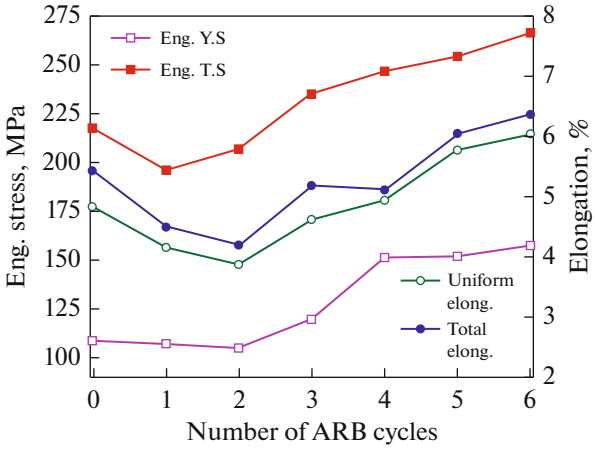

Fig. 10. Strength and elongation variations of composites during various ARB cycles.

In the present research, tensile properties improvement of the processed composites results not only from the above mentioned mechanisms but also from the reinforcing role of Ni, Cu, and Mg fragments in the composites [8]. With increasing the number of ARB cycles, the homogeneous distribution of these fragments in the Al matrix is achieved, and leads to the increase of the strength of the composites [1, 18].

Variation of tensile properties with the number of ARB cycles are plotted in Fig. 10. As is seen, uniform and total elongation of composites decreased at first and second ARB cycles and then started to increase to last cycle and finally reached 6 and 6.4% in the last cycle from 5 and 5.5% in primary sandwiches, respectively. In order to maintain a useful understanding of strength in Al/Cu/Mg/Ni composites which are produced through ARB process, specific strength is measured. Archimedes principle was employed to measure mean specific density of composites using ASTM 373-88R9 standard. Mean density of the composite was 3.16 g/cm^3 and, therefore, strength-to-density was obtained 84.14—about 3.25 times more than that of commerciality pure as-received Al (25.92).

3.3. Fractography

Figure 11 illustrates SEM micrographs from tensile fracture surface of the composites. It is obvious that according to dimple shapes, fracture type of the composites is ductile and fracture mode has changed from normal (in primary sandwich) to shear-and-normal (in 6th ARB cycle). In other words, on the fracture

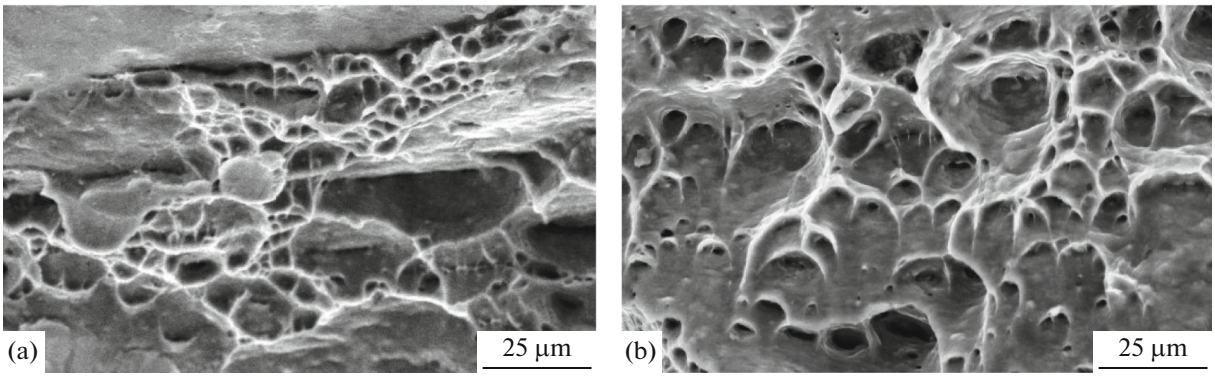

Fig. 11. Dimples in SEM micrograph of tensile fracture surface of Al/Cu/Mg/Ni multilayer composites at (a) primary sandwich and (b) 6th ARB cycle.

surface of the composite prepared by six cycles the occurrence of facets and dimples can be found simultaneously, which implies the existence of mixed ductile and brittle mode of fracture. This can be understood from the shape of dimples that have changed from normal to a mixture of normal and shear dimples. This separation model was seen in some other studies of materials under large strain deformation [22]. This is due to that with increasing ARB cycles from primary sandwich to 6th ARB cycle, deformation-induced bond strength between composite layers has increased due to increasing interdiffusion between layers [23]. Therefore, as is mentioned and shown in EDX profiles (Fig. 4), increasing the number of ARB cycles has increased interdiffusion of layers and this phenomenon has increased strength of composites due to differences in modulus of elasticity and strength of matrix metal and reinforcing particles.

4. CONCLUSIONS

At the present study, Al/Cu/Mg/Ni multilayer metal matrix composites were fabricated in 6 cycles of ARB process and corresponding mechanical and metallurgical properties are evaluated. The main results obtained are as follows:

(1) The multilayer Al/Cu/Mg/Ni composite was successfully processed via ARB process. With increasing of ARB cycles, the distribution of Cu, Mg, and Ni layers in the Al matrix increased and after 6 cycles a composite with homogeneously dispersed layers was produced.

(2) Vickers microhardness of different layers increased by increasing ARB cycles due to increasing dislocation densities during severe plastic deformation process of layers.

(3) Tensile strength of the composite decreased at the first ARB cycle due to necking and fracturing of Cu and Ni layers and then started to increase till final (6th) ARB cycle. Also, the elongation decreased from primary sandwich to 2nd ARB cycle and then increased in the next cycles to 6th (final) ARB cycle.

(4) Measurement of specific strength which is defined as strength-to-density ratio showed that specific strength of the composite has become about 3.25 times higher than that of matrix metal (Al).

(5) Fracture mode has changed from normal in the primary sandwich to normal-and-shear in 6th ARB cycle, and due to the observed dimples in both conditions, it can be concluded that fracture mode in the composites was ductile.

ACKNOWLEDGMENTS

The authors would like to thank the research board of Sahand University of Technology for the provision of research facilities used in this work.

FUNDING

The authors are grateful of Iran Nanotechnology Initiative Council for support and sponsorship on the master thesis and current research.

REFERENCES

1. M. Tayyebi and B. Eghbali, "Study on the microstructure and mechanical properties of multilayer Cu/Ni composite processed by accumulative roll bonding," Mater. Sci. Eng., A **559**, 759–764 (2013).
2. R. N. Dehsorkhi, F. Qods, and M. Tajally, "Investigation on microstructure and mechanical properties of Al–Zn composite during accumulative roll bonding (ARB) process," Mater. Sci. Eng., A **530**, 63–72 (2011).
3. V. Viswanathan, L. Laha, K. Balani, A. Agarwal, and S. Seal, "Challenges and advances in nanocomposite processing techniques," Mater. Sci. Eng., R **54**, 121–285 (2006).
4. A. K. Padap, G. P. Ghaudhari, S. K. Nath, and V. Pancholi, "Ultrafine-grained steel fabricated using warm multiaxial forging: Microstructure and mechanical properties," Mater. Sci. Eng., A **527**, 110–117 (2009).

5. L. Li, K. Nagai, and F. Yin, "Progress in cold roll bonding of metals," Sci. Technol. Adv. Mater. **9**, 023001 (2008).
6. A. Shabani, M. R. Toroghinejad, and A. Shafyei, "Fabrication of Al/Ni/Cu composite by accumulative roll bonding and electroplating processes and investigation of its microstructure and mechanical properties," Mater. Sci. Eng., A **558**, 386–393 (2012).
7. K. Brunelli, L. Peruzzo, and M. Dabal, "The effect of prolonged heat treatments on the microstructural evolution of Al/Ni intermetallic compounds in multi layered composites," Mater. Chem. Phys. **149–150**, 350–358 (2015).
8. L. Ghalandari, M. M. Mahdavian, and M. Reihanian, "Microstructure evolution and mechanical properties of Cu/Zn multilayer processed by accumulative roll bonding (ARB)," Mater. Sci. Eng., A **593**, 145–152 (2014).
9. J. S. Carpenter, S. C. Vogel, J. E. LeDonne, D. L. Hammon, I. J. Beyerlein, and N. A. Mara, "Bulk texture evolution of Cu–Nb nanolamellar composites during accumulative roll bonding," Acta Mater. **60**, 1576–1586 (2012).
10. H. S. Liu, B. Zhang, and G. P. Zhang, "Microstructures and mechanical properties of Al/Mg alloy multilayered composites produced by accumulative roll bonding," J. Mater. Sci. Technol. **27**, 15–21 (2011).
11. M. Talebian and M. Alizadeh, "Manufacturing Al/steel multilayered composite by accumulative roll bonding and the effects of subsequent annealing on the microstructural and mechanical characteristics," Mater. Sci. Eng., A **590**, 186–193 (2014).
12. S. Roy, B. R. Nataraj, S. Suwas, S. Kumar, and K. Chattopadhyay, "Accumulative roll bonding of aluminum alloys 2219/5086 laminates: Microstructural evolution and tensile properties," Mater. Des. **36**, 529–539 (2012).
13. Y. F. Sun, N. Tsuji, H. Fujii, and F. S. Li, "Cu/Zr nanoscaled multi-stacks fabricated by accumulative roll bonding," J. Alloys Compd. **504**, 443–447 (2010).
14. G. Min, J. M. Lee, S. B. Kang, and H. W. Kim, "Evolution of microstructure for multilayered Al/Ni composites by accumulative roll bonding process," Mater. Lett. **60**, 3255–3259 (2006).
15. M. Eizadjou, H. D. Manesh, and K. Janghorban, "Microstructure and mechanical properties of ultrafine grains (UFGs) aluminum strips produced by ARB process," J. Alloys Compd. **474**, 406–415 (2009).
16. N. Tsuji, Y. Ito, Y. Saito, and Y. Minamino, "Strength and ductility of ultrafine grained aluminum and iron produced by ARB and annealing," Scr. Mater. **47**, 893–899 (2002).
17. F. J. Humphreys and M. Hatherly, *Recrystallization and Related Annealing Phenomena*, 2nd ed. (Elsevier, Oxford, 2004).
18. K. Wu, H. Chang, E. Maawad, W. M. Gan, H. G. Brokmeier, and M. Y. Zheng, "Microstructure and mechanical properties of the Mg/Al laminated composite fabricated by accumulative roll bonding," Mater. Sci. Eng., A **527**, 3073–3078 (2010).
19. M. Alizadeh, M. H. Paydar, and F. Jazi Sharifian, "Structural evaluation and mechanical properties of nanostructured Al/B4C composite fabricated by ARB process," Composites, Part B **44**, 339–343 (2013).
20. N. Hansen, X. Huang, R. Ueji, and N. Tsuji, "Structure and strength after large strain deformation," Mater. Sci. Eng., A **387**, 191–194 (2004).
21. Y. M. Wang and E. Ma, "Three strategies to achieve uniform tensile deformation in a nanostructured metal," Acta Mater. **52**, 1699–1709 (2004).
22. M. Shaarbaf and M. R. Toroghinejad, "Nano-grained copper strip produced by accumulative roll bonding process," Mater. Sci. Eng., A **473**, 28–33 (2008).
23. K. S. Lee, D. H. Yoon, H. K. Kim, Y. N. Kwon, and Y. S. Lee, "Effect of annealing on the interface microstructure and mechanical properties of a STS–Al–Mg 3-ply clad sheet," Mater. Sci. Eng., A **556**, 319–330 (2012).